Solar Physics
DOI: 10.1007/•••••-•••-•••-••••-•

A Statistical Study of Distant Consequences of Large Solar Energetic Events

Carolus J. Schrijver[1] · **Paul A. Higgins**[1,2]

Abstract Large solar flares and eruptions may influence remote regions through perturbations in the outer-atmospheric magnetic field, leading to causally related events outside of the primary or triggering eruptions that are referred to as "sympathetic events". We quantify the occurrence of sympathetic events using the full-disk observations by the *Atmospheric Imaging Assembly* onboard the *Solar Dynamics Observatory* associated with all flares of GOES class M5 or larger from 01 May 2010 through 31 December 2014. Using a superposed-epoch analysis, we find an increase in the rate of flares, filament eruptions, and substantial sprays and surges more than 20° away from the primary flares within the first four hours at a significance of 1.8 standard deviations. We also find that the rate of distant events drops by two standard deviations, or a factor of 1.2, when comparing intervals between 4 hours and 24 hours before and after the start times of the primary large flares. We discuss the evidence for the concluding hypothesis that the gradual evolution leading to the large flare and the impulsive release of the energy in that flare both contribute to the destabilization of magnetic configurations in distant active regions and quiet-Sun areas. These effects appear to leave distant regions, in an ensemble sense, in a more stable state, so that fewer energetic events happen for at least a day following large energetic events.

Keywords: Flares; Coronal mass ejections; Corona; Sun: magnetic field

1. Introduction

Over the past decades, full-disk chromospheric and coronal imagers have revealed a great deal of activity in the solar outer atmosphere, with much attention going to the energetic phenomena of flares and eruptions. Evidence is accumulating rapidly that coronal perturbations have a long reach across the Sun as instrument cadence, sensitivity, and wavelength coverage increase, in particular in recent years with the deployment of the *Atmospheric Imaging Assembly* (AIA: Lemen

[1] Lockheed Martin Advanced Technology Center, 3251 Hanover St., Palo Alto, USA, email: schrijver@lmsal.com,
[2] School of Physics, Trinity College Dublin, College Green, Dublin, Ireland

et al., 2012) onboard the *Solar Dynamics Observatory* (SDO: Pesnell, Thompson, and Chamberlin, 2012). This includes the perturbations and deformations of the coronal magnetic field associated with the initial phases of coronal mass ejections (CMEs), involving various wave and wave-like processes (*e.g.* Downs *et al.*, 2012; Liu *et al.*, 2012; Patsourakos and Vourlidas, 2012; Nitta *et al.*, 2013; Liu and Ofman, 2014, and references therein) and the slower deformation of high magnetic field either by distant flux emergence or by nearby eruptions (*e.g.* Schrijver and Title, 2011; Schrijver *et al.*, 2013, and references therein). With the advances in observational capabilities, together with increasing computational tools, answers to questions about couplings between energetic solar events may be coming within reach (*e.g.* Török *et al.*, 2011; Jacobs and Poedts, 2012; Lynch and Edmondson, 2013), but it remains a challenge to observers to establish the frequency at which significant long-range interactions occur.

Among the interactions considered, one commonly referred to as "sympathy" has received particular attention, because it relates both to the understanding of what is involved in the destabilization of magnetic configurations and to the development of heliospheric events such as CMEs and solar energetic particle (SEP) events (see Harrison *et al.*, 2012, for an extensive discussion on a sample set of interacting events). "Sympathy" — defined here as the coupling of events in distinct solar regions through the modification of the atmospheric magnetic field — can occur either by the gradual evolution of the surface magnetic field (through emergence, displacement, or cancellation) or by relatively sudden changes that are associated with explosive and/or eruptive events. The interactions induced by the gradual changes associated with flux emergence have been studied, for example by Fu and Welsch (2015, and references therein). They conclude that "newly emerging regions produce a significant increase in the occurrence rate of X- and M-class flares in pre-existing regions" other than close to, or at, the location of new flux emergence (where they note the effect is significant at about the level of two standard deviations in the event counts, assuming Poisson statistics). In this case, the stored (free) energy of the large flare is released from an active region as its field configuration is altered by the gradual evolution of one or more regions external to the destabilized field, either by induction alone or by the eventual reconnection-enabled field reconfiguration. Such couplings are, of course, not limited to active regions, but may – as noted by Fu and Welsch (2015) – also affect quiet-Sun configurations including large filaments and the CMEs that their destabilization may induce.

On shorter time scales, eruption-related disturbances in the coronal field may be involved in sympathy. These disturbances may be transient as in the case of waves, or irreversible as may happen during large coronal mass ejections, or a mixture of both. One example, studied both on the Sun and in virtual settings, is the coupling between adjacent quiet-Sun filaments, where the eruption of one plausibly leads to the eruption of another one (*e.g.* Schrijver and Title, 2011; Török *et al.*, 2011).

The full-Sun, high-cadence view of the solar corona offered by SDO/AIA has shown many examples in which couplings between events could be inferred to exist, either through waves or to lasting field perturbations. A sample of such events was described in detail by Schrijver *et al.* (2013). However, although

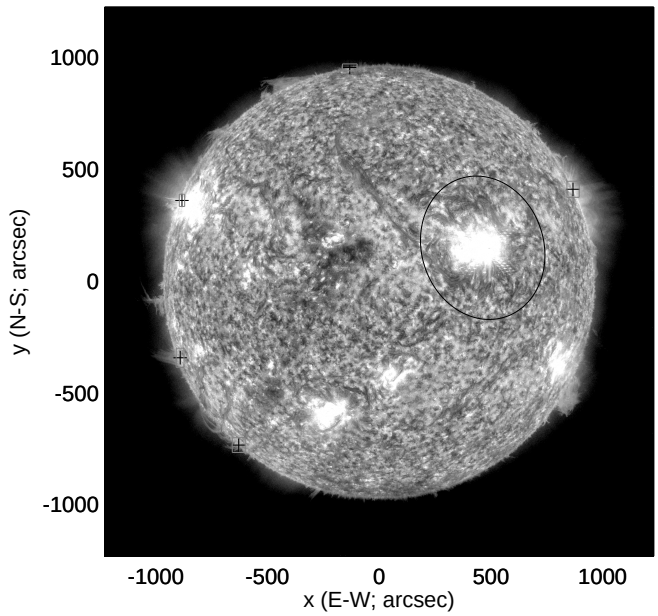

Figure 1. Image taken by SDO/AIA in the 304 Å passband on 07 September 22:35 UT, exposing during an X1.8 flare (SOL2011-09-07T22:32:32L223C076). A distance from the flare's center of 20 heliocentric degrees is shown by the black circle projected onto the Sun as viewed from SDO's perspective. Five other events were flagged within 24 hours of this flare, shown by pluses and their bounding boxes in grey, in this case all near or at the limb.

the couplings in many cases appear plausible, the statistical evidence about the frequency and impact of such couplings needed work. Fu and Welsch (2015) now provide such information on couplings between flux emergence in one location and flaring in another. In this study, we look at couplings between large impulsive events (associated with flares of magnitude M5 or larger) in one location and any substantial energetic event elsewhere on the visible hemisphere on the Sun.

2. Observations and Results

We start from the list of flares of GOES class M5 or larger that occurred within 70° from disk center in the period of post-commissioning SDO observations (starting on 01 May 2010) through 31 December 2014. For each flare, we inspected SDO/AIA 304 Å image sequences for flares, filament eruptions, and large surges/sprays that occurred anywhere on the disk and over the limb for periods spanning at least 24 hours before and after the start times of each selected large flare. For each such identified event, we recorded the central position, bounding box, estimated start time, and whether the event was a flare and/or eruption, and whether the event occurred in active- or quiet-Sun settings. We also inspected image sequences of the *Large Angle and Spectrometric COronagraph* (LASCO:

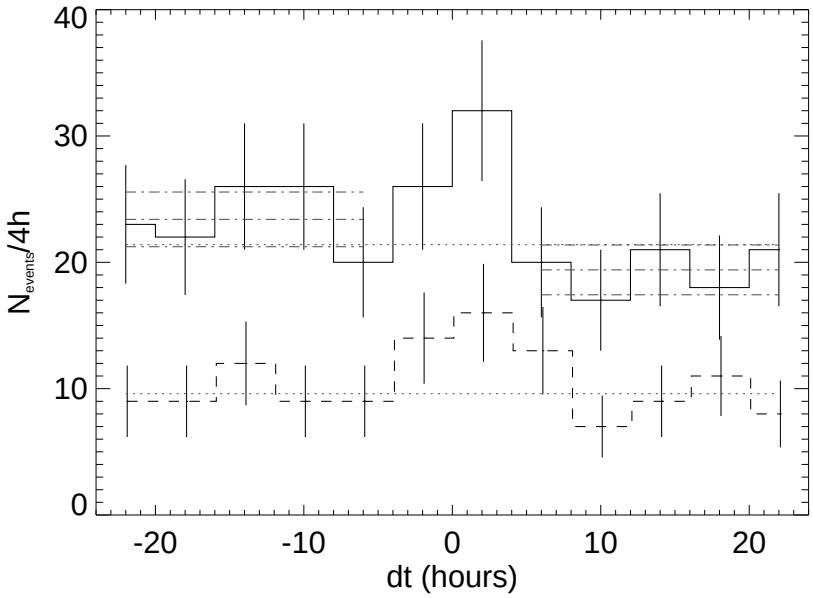

Figure 2. Superposed-epoch histogram of the number of solar events (per four-hour interval) around the time of flares of GOES class M5 or larger in the period from 01 May 2010 through 31 December 2014 that occurred within 70 heliocentric degrees from disk center. The solid histograms shows the number distribution for all events (flares and eruptions) on the visible hemisphere or beyond the limb with central coordinates more than 20 heliocentric degrees away from the flare location. The dashed histogram shows the same but for all events originating in quiet-Sun regions. The uncertainty bars (slightly offset for the quiet-Sun events to avoid overlap) assume Poisson statistics. The dotted lines show the average event rates for the two samples over the 32 hour intervals excluding times within four hours of the flare peak times. The grey dash–dotted lines show the averages (and the one σ ranges) from four hours to 24 hours before and after the flare start times, respectively.

Brueckner *et al.*, 1995) on the *SOlar and Heliospheric Observatory* (SOHO) image sequences to assess whether the large flares appeared to be associated with a CME.

The selected reference events are listed in Table 1, identified using the IAU SOL target naming convention (Leibacher *et al.*, 2010). In order to quantify the frequency of long-range couplings, we identified other flares and eruptions well away from the flaring active region. We set a threshold of 20° for the minimum distance between the flare site and the central position of any other event (see Figure 1 for an example of this). The results are sorted chronologically within each of three groups in Table 1. The first set contains the 18 flares with no other events identified elsewhere on the Sun at least 20° from the flare site as seen by SDO/AIA within 24 hours on either side of the flare. The second set, with 13 flares, contains those flares with a single other event meeting the above criteria. The third set of 16 flares lists those with two or more events flagged.

Figure 2 is a superposed epoch rendering of the frequency of observed events as function of time difference. It summarizes the distribution of the number of

Table 1. Selected flares and association with a CME (in SOHO/LASCO data) differentiated the number of events flagged in 304 Å data over 20° from the flare site, respectively, within 24 hours of flare start times. Column 3: plane of the sky velocities [v_C] of CME. Column 4: velocities [V_L] of large-scale propagating fronts (LCPF; from Nitta *et al.*, 2013), with values for events outside of the interval in the original study shown between brackets as determined later with the same procedure, or dots if no LCPF is observed. If a distant AIA event occurs within four hours following the flare, an asterisk is added to the last column.

SOL	Class	$v_{[}$(km s^{-1}]	v_L [km s^{-1}]	Notes
18 flares with no distant events within 24 hours:				
SOL2011-07-30T02:03:44L001C090	M9.3	-	383	no CME
SOL2011-08-03T13:16:48L333C074	M6.0	610	604	CME
SOL2011-08-04T03:40:48L331C071	M9.3	1315	910	CME
SOL2011-08-09T07:48:16L296C073	X6.9	1610	743	CME
SOL2012-03-05T02:30:24L302C073	X1.1	594	915	CME
SOL2012-03-07T00:02:08L329C090	X5.4	1825	828	CME
SOL2012-03-07T01:05:04L317C068	X1.3	"	789	CME (?)
SOL2012-03-10T17:14:40L280C090	M8.4	491	522	CME
SOL2012-07-04T09:46:40L209C110	M5.3	-	-	no CME
SOL2012-10-23T03:13:04L167C090	X1.8	-	-	no CME
SOL2012-11-13T01:58:24L252C090	M6.0	611	-	CME
SOL2013-10-25T07:53:36L001C090	X1.7	587	[973]	CME
SOL2013-10-25T14:51:44L358C090	X2.1	1081	[1314]	CME
SOL2013-11-05T22:06:56L162C102	X3.3	562	...	CME
SOL2014-01-07T10:08:00L093C103	M7.2	451	...	CME
SOL2014-01-30T15:47:12L100C103	M6.6	780	...	CME
SOL2014-03-29T17:36:00L145C079	X1.0	528	[1561]	CME
SOL2014-04-02T13:17:52L010C076	M6.5	1471	[703]	CME
13 flares with one distant event within 24 hours:				
SOL2011-09-06T22:12:16L227C076	X2.1	575	1246	CME *
SOL2011-09-08T15:32:16L226C076	M6.7	214	649	no(?) CME
SOL2011-09-24T09:21:04L278C078	X1.9	1936	1129	CME
SOL2011-09-24T12:33:04L337C090	M7.1	1915	640	CME *
SOL2012-05-10T04:10:40L179C077	M5.7	-	-	no CME *
SOL2012-07-05T11:38:40L108C112	M6.1	-	-	no CME
SOL2012-07-06T23:01:20L156C090	X1.1	1828	-	CME
SOL2012-07-12T15:36:32L082C105	X1.4	843	542	CME *
SOL2013-10-24T00:21:20L010C100	M9.3	-	[594]	no CME *
SOL2013-10-28T01:40:16L031C086	X1.0	695	[1403]	CME
SOL2013-11-08T04:20:16L163C104	X1.1	497	...	CME *
SOL2014-01-07T18:03:44L100C090	X1.2	1830	[1036]	CME *
SOL2014-02-04T03:56:48L105C104	M5.2	-	...	no CME *
16 flares with two or more distant events within 24 hours:				
SOL2011-09-06T01:34:56L227C076	M5.3	782	1041	CME *
SOL2011-09-07T22:32:32L223C076	X1.8	792	1307	CME *
SOL2011-09-24T20:28:48L332C090	M5.8	-	-	no CME *
SOL2011-09-25T04:30:56L281C079	M7.4	788	740	CME *
SOL2011-11-03T20:16:00L101C068	X1.9	-	-	no CME *
SOL2012-01-23T03:37:36L208C062	M8.7	2175	837	CME
SOL2012-03-09T03:21:36L301C090	M6.3	950	689	CME *
SOL2012-03-13T17:12:32L241C090	M7.9	1884	1022	CME *
SOL2012-07-02T10:43:12L209C107	M5.6	?	1234	CME *
SOL2012-07-28T20:43:44L173C115	M6.1	420	[546]	CME *
SOL2013-04-11T06:56:00L073C081	M6.5	861	[719]	CME *
SOL2013-05-15T01:25:20L296C078	X1.2	1366	...	CME *
SOL2013-11-01T19:46:08L262C101	M6.3	268	...	CME *
SOL2013-11-10T05:07:12L164C104	X1.1	682	...	CME *
SOL2013-12-31T21:45:36L226C106	M6.4	271	...	CME *
SOL2014-01-01T18:40:00L227C104	M9.9	236	...	CME

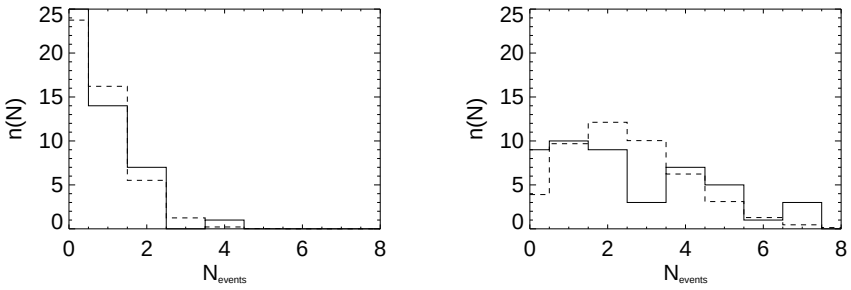

Figure 3. (left) Histogram of the number of events observed in the SDO/AIA 304 Å image sequences within four hours following, and more than 20° from, each selected M5-class flare or larger (solid). For comparison, a Poisson distribution with the same average number of events (0.7) is shown (dashed). (right) Same, but for events between 24 and 4 hours before the flares, and a Poisson distribution with average of 1.5 events.

flagged events that occurred more than 20° away from major flares. The diagram shows event counts in four-hour intervals within 24 hours of the reference times that are defined as the start times the GOES X-ray flares. The distributions suggest that there is an increased number of events in the four-hour interval immediately following large flares at about the 1.8 σ level; for the set of events occurring in quiet-Sun regions, a comparable difference is seen at about 1.6 σ (assuming Poisson statistics). For the full set of events, the mean event rate following flares appears to be somewhat lower well after the flares ($4-24$ hours) than in the corresponding interval before; the difference of about 1.7 standard deviations equals a ratio of 1.2 ± 0.2.

Figure 3 shows the distribution of the number of events within four hours following each large flare (solid) compared to a Poisson distribution of the same mean number of events (dashed). The second panel shows the same for an interval between 16 hours and 4 hours prior to the flare start time. Both cases are roughly compatible with the assumption of Poisson statistics. We may conclude that the majority of events present random waiting times, but we learn little from that in the context of this study.

The data summarized in Table 1 show that the fraction of M5 flares or larger with CMEs is 0.8, 0.6, and 0.8 for flares with zero, one, or more than one distant events within 24 hours of the flare peak time, *i.e.* there is no significant distinction in CME fraction as a function of the number of distant events. Average flare classes (using an averaging based on the values of the flare peak brightness as used in flare class, and specifying the standard deviation in the mean) are X (1.7±0.4), X (1.1±0.1), and M (9±1). Again, there is no significant difference in flare class given the number of distant events, particularly given the range of flare classes in each group.

The average "linear speeds" (from cdaw.gsfc.nasa.gov/CME_list/) and the associated standard deviations in the mean for CMEs are: $890 \pm 130\,\mathrm{km\,s^{-1}}$, $1150 \pm 250\,\mathrm{km\,s^{-1}}$, and $880 \pm 170\,\mathrm{km\,s^{-1}}$, respectively. There is no obvious trend in these averages as function of the number of distant events within four hours

from the flare start times, but "linear speed" is a plane-of-the-sky quantity and thus only in part informative about the actual propagation speeds of CMEs.

More informative about what happens in the lower corona may be the occurrence and properties of large-scale propagating fronts (LCPFs) that are associated with many eruptive events. Table 1 lists the velocities measured by Nitta *et al.* (2013) for events between April 2010 and January 2013, and some later events measured by N. Nitta (private communication, 2015) with the same algorithm: for zero, one, and two or more distant events within a four-hour time window, these velocities and the standard deviations in the mean are $854 \pm 98\,\mathrm{km\,s^{-1}}$, $905 \pm 127\,\mathrm{km\,s^{-1}}$, and $903 \pm 92\,\mathrm{km\,s^{-1}}$, respectively. We thus find no significant trend in the number of "sympathetic events" with velocity of the LCPF.

3. Discussion

The review of full-disk SDO/AIA 304 Å observations of 48 hour intervals centered on flares of class M5 or larger reveals that other flares, filament eruptions, and large sprays/surges that occur more than 20° away from the reference flare site have a marginally significant increase in their rate during the first four hours following the large reference flares. This interval is followed by a period of at least 20 hours during which the event rates elsewhere on the disk are likely to be somewhat reduced relative to the rate $4-24$ hours before the large reference flares.

Owing to the relatively weak solar cycle, the number of large flares was low, contributing to the fact that these results are statistically significant only at about the 1.7 to 1.8 standard deviation level. In view of the other evidence in support of "sympathy" between solar energetic events as discussed in Section 1, we note that the results from this study are consistent with the hypothesis that major flares may cause the destabilization of distant magnetic configurations. We consider it likely that the large flares and associated coronal perturbations do this by causing destabilization to occur earlier than would occur in the absence of such large flaring, *i.e.* by affecting primarily the timing of these events, and possibly also their occurrence in the first place.

The data not only show a moderately significant increase in distant–event rates within the first four hours following major flares, but also suggest a drop by about two standard deviations, or by a factor of about 1.2 ± 0.2, in distant–event rates when comparing intervals between four and 24 hours before and after the flares. We propose that this drop is associated in large part with the effects of flux emergence within the flaring region: Large flares are often associated with signatures of flux emergence within a pre-existing active region (*e.g.* Schrijver, 2007; Welsch and Li, 2008; Schrijver, 2009; Welsch *et al.*, 2009), and flux emergence enhances the probability of flaring in distant regions (Fu and Welsch, 2015). The decrease by a factor of about 1.2 in event rates between four and 24 hours before and after M5 flares or larger is roughly comparable to the relative change in flare frequencies (also M5 or larger) between three-day intervals before and after flux emergence of a factor of $1.2-1.7$ found by Fu

and Welsch (2015), being larger for samples restricted to larger emerging flux regions.

In conclusion, we propose a scenario with two components: the gradual evolution leading to large flares and the impulsive release of stored energy in the flare process jointly contribute to the destabilization of magnetic configurations, both in distant active regions and in quiet-Sun areas. The large impulsive events can lead to destabilization of relatively distant regions, leaving these in a lower energy or more stable state so that fewer energetic events happen for at least a day following the large primary events. Part of the drop in the rate of distant events before and after major flaring may also reflect that major flares occur towards the end of the emergence of a flux rope within active regions, but that aspect remains to be tested.

Acknowledgements This work was supported by NASA 's SDO/AIA contract (NNG04EA00C) to LMSAL. AIA is an instrument onboard the *Solar Dynamics Observatory*, a mission for NASA's Living With a Star program. Data are provided courtesy of NASA/SDO and the AIA science team. We thank George Lee for his help in reviewing and annotating the AIA observations, and Nariaki Nitta for applying his perturbation-tracking algorithm to some of the more recent large-scale propagating fronts.

Disclosure of Potential Conflicts of Interest

The authors declare that they have no conflicts of interest.

References

Brueckner, G.E., Howard, R.A., Koomen, M.J., Korendyke, C.M., Michels, D.J., Moses, J.D., Socker, D.G., Dere, K.P., Lamy, P.L., Llebaria, A., Bout, M.V., Schwenn, R., Simnett, G.M., Bedford, D.K., Eyles, C.J.: 1995, The Large Angle Spectroscopic Coronagraph (LASCO). *Solar Phys.* **162**, 357. DOI. ADS,

Downs, C., Roussev, I.I., van der Holst, B., Lugaz, N., Sokolov, I.V.: 2012, Understanding SDO/AIA Observations of the 2010 June 13 EUV Wave Event: Direct Insight from a Global Thermodynamic MHD Simulation. *Astrophys. J.* **750**, 134.

Fu, Y., Welsch, B.T.: 2015, Triggering of Remote Flares by Magnetic Flux Emergence. *ArXiv e-prints 1504.06633*.

Harrison, R.A., Davies, J.A., Möstl, C., Liu, Y., Temmer, M., Bisi, M.M., Eastwood, J.P., de Koning, C.A., Nitta, N., Rollett, T., Farrugia, C.J., Forsyth, R.J., Jackson, B.V., Jensen, E.A., Kilpua, E.K.J., Odstrcil, D., Webb, D.F.: 2012, An Analysis of the Origin and Propagation of the Multiple Coronal Mass Ejections of 2010 August 1. *Astrophys. J.* **750**, 45.

Jacobs, C., Poedts, S.: 2012, A Numerical Study of the Response of the Coronal Magnetic Field to Flux Emergence. *Solar Phys.* **280**, 389. DOI. ADS,

Leibacher, J., Sakurai, T., Schrijver, C.J., van Driel-Gesztelyi, L.: 2010, Solar Observation Target Identification Convention for use in Solar Physics. *Solar Phys.* **263**, 1. DOI. ADS,

Lemen, J.R., Title, A.M., Akin, D.J., Boerner, P.F., Chou, C., Drake, J.F., Duncan, D.W., Edwards, C.G., Friedlaender, F.M., Heyman, G.F., Hurlburt, N.E., Katz, N.L., Kushner, G.D., Levay, M., Lindgren, R.W., Mathur, D.P., McFeaters, E.L., Mitchell, S., Rehse, R.A., Schrijver, C.J., Springer, L.A., Stern, R.A., Tarbell, T.D., Wuelser, J.-P., Wolfson, C.J., Yanari, C., Bookbinder, J.A., Cheimets, P.N., Caldwell, D., Deluca, E.E., Gates, R., Golub, L., Park, S., Podgorski, W.A., Bush, R.I., Scherrer, P.H., Gummin, M.A., Smith,

P., Auker, G., Jerram, P., Pool, P., Soufli, R., Windt, D.L., Beardsley, S., Clapp, M., Lang, J., Waltham, N.: 2012, The Atmospheric Imaging Assembly (AIA) on the Solar Dynamics Observatory (SDO). *Solar Phys.* **275**, 17. DOI. ADS,

Liu, W., Ofman, L.: 2014, Advances in Observing Various Coronal EUV Waves in the SDO Era and Their Seismological Applications (Invited Review). *Solar Phys.* **289**, 3233. DOI. ADS,

Liu, W., Ofman, L., Nitta, N.V., Aschwanden, M.J., Schrijver, C.J., Title, A.M., Tarbell, T.D.: 2012, Quasi-periodic Fast-mode Wave Trains within a Global EUV Wave and Sequential Transverse Oscillations Detected by SDO/AIA. *Astrophys. J.* **753**, 52.

Lynch, B.J., Edmondson, J.K.: 2013, Sympathetic Magnetic Breakout Coronal Mass Ejections from Pseudostreamers. *Astrophys. J.* **764**, 87.

Nitta, N.V., Schrijver, C.J., Title, A.M., Liu, W.: 2013, Large-scale Coronal Propagating Fronts in Solar Eruptions as Observed by the Atmospheric Imaging Assembly on Board the Solar Dynamics Observatory - an Ensemble Study. *Astrophys. J.* **776**, 58. DOI. ADS,

Patsourakos, S., Vourlidas, A.: 2012, On the Nature and Genesis of EUV Waves: A Synthesis of Observations from SOHO, STEREO, SDO, and Hinode (Invited Review). *Solar Phys.* **281**, 187.

Pesnell, W.D., Thompson, B.J., Chamberlin, P.C.: 2012, The Solar Dynamics Observatory (SDO). *Solar Phys.* **275**, 3. DOI. ADS,

Schrijver, C.J.: 2007, A Characteristic Magnetic Field Pattern Associated with All Major Solar Flares and Its Use in Flare Forecasting. *Astrophys. J. Lett.* **655**, 117.

Schrijver, C.J.: 2009, Driving major solar flares and eruptions: A review. *Advances in Space Research* **43**, 739.

Schrijver, C.J., Title, A.M.: 2011, Long-range magnetic couplings between solar flares and coronal mass ejections observed by SDO and STEREO. *Journal of Geophysical Research (Space Physics)* **116**(A15), 4108.

Schrijver, C.J., Title, A.M., Yeates, A.R., DeRosa, M.L.: 2013, Pathways of Large-scale Magnetic Couplings between Solar Coronal Events. *Astrophys. J.* **773**, 93.

Török, T., Panasenco, O., Titov, V.S., Mikić, Z., Reeves, K.K., Velli, M., Linker, J.A., De Toma, G.: 2011, A Model for Magnetically Coupled Sympathetic Eruptions. *Astrophys. J., Lett.* **739**, L63.

Welsch, B.T., Li, Y.: 2008, On the Origin of Strong-Field Polarity Inversion Lines. In: Howe, R., Komm, R.W., Balasubramaniam, K.S., Petrie, G.J.D. (eds.) *Subsurface and Atmospheric Influences on Solar Activity*, **CS-383**, Astron. Soc. Pacific, San Francisco, 429.

Welsch, B.T., Li, Y., Schuck, P.W., Fisher, G.H.: 2009, What is the Relationship Between Photospheric Flow Fields and Solar Flares? *Astrophys. J.* **705**, 821.